Acta Cryst E CRYSTALLOGRAPHIC COMMUNICATIONS
ISSN 2056-9890

Synthesis, optical properties and crystal structure of (*E*,*E*)-1,3-(3,4:9,10-dibenzododeca-1,11-diene-5,7-diyne-1,12-diyl)benzene

Hikaru Watanabe,[a] Takuma Sato,[a] Michiki Sumita,[a] Mei Shiroyama,[a] Daichi Sugawara,[a] Tomoki Tokuyama,[a] Yasuhiro Okuda,[a] Kan Wakamatsu,[b] Haruo Akashi[c] and Akihiro Orita[a]*

[a]Department of Applied Chemistry, Okayama University of Science, 1-1 Ridai-cho, Kita-ku, Okayama 700-0005, Japan, [b]Department of Chemistry, Okayama University of Science, 1-1 Ridai-cho, Kita-ku, Okayama 700-0005, Japan, and [c]Research Institute of Frontier Science and Technology, Okayama University of Science, 1-1 Ridai-cho, Kita-ku, Okayama 700-0005, Japan. *Correspondence e-mail: orita@ous.ac.jp

Received 2 June 2023
Accepted 14 July 2023

Edited by S. Parkin, University of Kentucky, USA

Keywords: crystal structure; expanded π-system; dehydrobenzannulene; reductive desulfonylation.

CCDC reference: 2252157

Supporting information: this article has supporting information at journals.iucr.org/e

The dehydrobenzannulene (*E*,*E*)-1,3-(3,4:9,10-dibenzododeca-1,11-diene-5,7-diyne-1,12-diyl)benzene, $C_{26}H_{16}$, was successfully synthesized *via* photocatalyst-assisted stereoselective reductive desulfonylation of 1,3-bis{1-phenylsulfonyl-2-[2-(trimethylsilylethynyl)phenyl]ethenyl}benzene, $C_{44}H_{42}O_4S_2Si_2$, and subsequent desilylative cyclization of the resulting (*E*,*E*)-bis-silyl-protected dienyne, $C_{32}H_{34}Si_2$. The structure of the dehydrobenzannulene thus obtained was confirmed by single-crystal X-ray analysis; three benzene rings are connected to one another by a 1,3-butadiynylene and a pair of ethenylene arrays. Although the π-system expanded efficiently in the dehydrobenzannulene, it was observed that the butadiynylene and ethenylene arrays were strained, showing smaller [171.3 (2)–172.6 (2) °] and larger bond angles [122.5 (2)–131.9 (2)°] than the conventional bond angles, respectively. In $CHCl_3$, the dehydrobenzannulene showed the longest absorption band at 377 nm. When irradiated by UV light, it emitted fluorescence at 468 nm ($\Phi_F = 0.26$) and 504 nm ($\Phi_F = 0.24$) in $CHCl_3$ and in the powdered state, respectively.

1. Chemical context

Dehydrobenzannulenes (DBAs) attract intensive attention because they often show new functionality for π-expanded compounds, such as a novel π–π interaction mode in fluoroarylene-DBA (Karki *et al.*, 2022), guest-dependent structure-transformative DBA inclusion crystals (Shigemitsu *et al.*, 2012), and a synthetic intermediate of [6.8]$_3$cyclacene (Esser *et al.*, 2008). In the syntheses of DBAs, ethenylene and ethynylene arrays are often used to connect aromatic rings to one another. For example, 1,3-(3,4:9,10-dibenzododeca-1,11-diene-5,7-diyne-1,12-diyl)benzene, $C_{26}H_{16}$, (**1**), is composed of three phenyl rings, a single butadienylene and a couple of ethenylene arrays. The synthesis of **1** was accomplished in 1985 (Ojima *et al.*, 1985). The synthetic route of **1** reported by Ojima was rather straightforward, and the desired dehydrobenzannulene **1** were successfully obtained. However, while the formation of (*E*,*E*)-**1** was spectroscopically confirmed, X-ray single crystallographic analysis has not yet been performed because of a poor chemical yield of (*E*,*E*)-**1** in Ojima's route. Recently we established an (*E*)-stereoselective synthesis of diarylethene *via* photocatalyst-assisted reductive desulfonylation of the corresponding diarylethenyl sulfone under irradiation by visible light (Watanabe *et al.*, 2020, 2021).

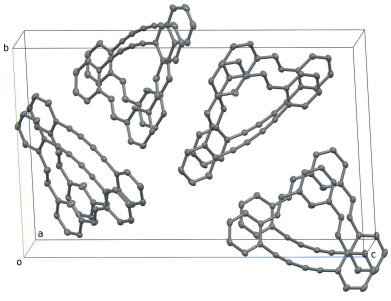

It was found out that this protocol could produce (*E*,*E*)-**1** efficiently in a pure form. This work reports the synthesis of the dehydrobenzannulene (*E*,*E*)-**1** and its single-crystal X-ray structure together with *UV* absorption and photoluminescence optical properties of (*E*,*E*)-**1** in $CHCl_3$ solution and in the solid state.

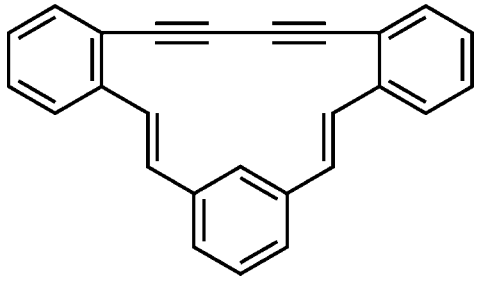

2. Structural commentary

The core structure of (*E*,*E*)-**1** is a 15-membered ring in which three phenylene rings are connected to one another by a 1,3-butadiynylene and a pair of (*E*)-ethenylene arrays (Fig. 1). Although the π-system in the 15-membered ring efficiently expands, there are slight twists observed in the π-systems between the (*E*)-ethenylene units and the connected phenylene units: *e.g.* C19—C18—C20—C21 = −10.5 (4)° and C20—C21—C22—C23 = 13.1 (4)°. In the 1,3-butadiynylene array, triple bonds C2≡C3 [1.204 (3) Å] and C4≡C5 [1.199 (3) Å] are remarkably shorter than the central single bond C3—C4 [1.374 (3) Å] and terminal single bonds C1—C2 [1.434 (3) Å] and C5—C6 [1.439 (3) Å]. The former single bond, C3—C4, is shorter by 0.06 Å than the latter because of the strong π-conjugation between ethynylene moieties. In the pair of phenylenes, which are *ortho*-fused to the 15-membered ring (C1–C26 and C6–C11), the aromatic C—C junction bonds C1—C22 and C6—C11 are longer than the other phenylene C—C bonds [1.414 (3) Å and 1.416 (3) Å *vs* 1.378 (4)–1.398 (3) Å] while in the *meta*-fused phenylene ring (C14–C19), all the aromatic C—C bonds are essentially identical in length [1.387 (3)–1.393 (3) Å]. With respect to bond angles in the 15-membered ring, the *sp* carbons of the 1,3-butadiynylene moiety show somewhat smaller bond angles than the ideal value of 180°, whereas the sp^2 carbons in the pair of (*E*)-ethenylene arrays show bond angles larger than 120°. In the 1,3-butadiynylene moiety, the inner *sp* carbons (C3 and C4) have *ca* 0.6° smaller bond angles than the outer (C2 and C5): *e.g.* C2—C3—C4 = 172.0 (2)° *vs* C1—C2—C3 = 172.6 (2)°. In the (*E*)-ethenylene moieties, C12 and C21 show *ca* 9.0° larger bond angles than C13 and C20: *e.g.* C11—C12—C13 = 131.9 (2) ° *vs* C12—C13—C14 = 122.5 (2)°.

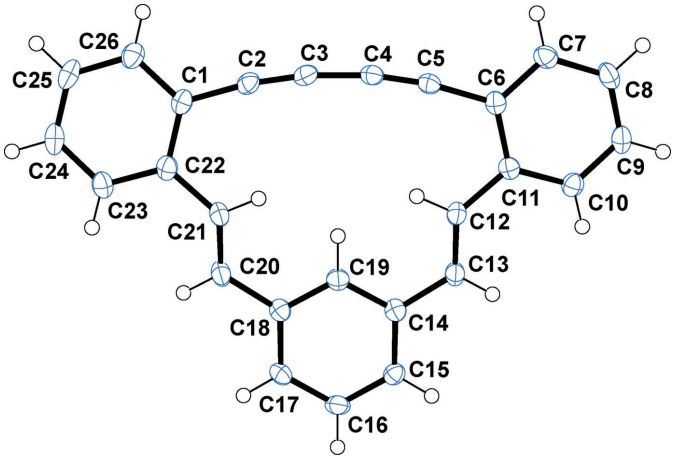

Figure 1
The molecular structure of (*E*,*E*)-**1** with displacement ellipsoids drawn at the 50% probability level.

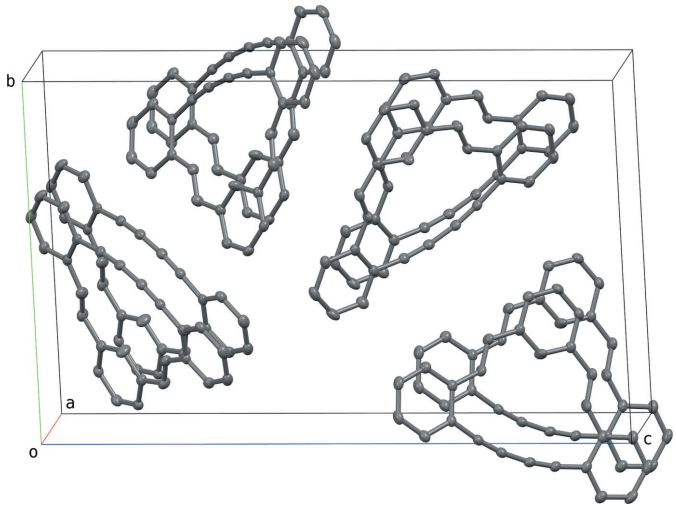

Figure 2
A partial packing plot of (*E*,*E*)-**1** viewed approximately down the crystallographic *a*-axis.

3. Supramolecular features

In the crystal, (*E*,*E*)-**1** molecules form columnar structures that extend along the *a*-axis direction in which the interlayer distance is 3.3639 (9) Å (calculated as the perpendicular distance from the mid-point of the 15-membered ring to the mean plane through the corresponding ring of an adjacent molecule in the stack), indicating an efficient intermolecular attractive interaction through π–π stacking (Fig. 2). The columns in which the (*E*,*E*)-**1** molecules are stacked are densely packed by van der Waals interactions.

4. Database survey

A search of the Cambridge Structural Database (version 5.43, November 2021 with updates to March 2022; Groom *et al.*, 2016) suggests the (*E*,*E*)-1,3-(3,4:9,10-dibenzododeca-1,11-diene-5,7-diyne-1,12-diyl)benzene [(*E*,*E*)-**1**] structure is unprecedented, although the first synthesis of (*E*,*E*)-**1** and its spectroscopic assignment have been reported (Ojima *et al.*, 1985). The 1,4-diphenyl-1,3-butadiyne fragment in analogous DBA is, however, more common, with more than ten examples reported, including the close relative of tribenzotetrayne DBA (refcode EKIMAM; Tobe *et al.*, 2003). The 1,3-bis(phenyl-

ethenyl)benzene fragment in analogous DBA is also common, with more than ten examples reported including the close relative of metacyclophanetrienes (GOBJIR and GOGMAR; Esser *et al.*, 2008).

5. Synthesis and crystallization

The dehydrobenzannulene **1** was synthesized from **2** in five steps (Fig. 3). The starting disulfone **2** and π-expanded pyrene photocatalyst **7** were prepared according to the literature (Orita *et al.*, 2006; Watanabe *et al.*, 2021, respectively). A consecutive treatment of **2** with BuLi, 2-bromobenzaldehyde, and acetic anhydride gave **3** in 94% yield as a diastereomeric mixture. The diacetate **3** was successfully converted to **4** in a 94% yield by treatment with *t*-BuOK, and the resulting dibromobis(sulfonylethenyl)benzene **4** was transformed to **5** with a 69% yield *via* Sonogashira–Hagihara coupling with trimethylsilylethyne (Watanabe *et al.*, 2020). Subsequently our original photocatalyst-assisted reductive desulfonylation was applied to bis(1-phenylsulfonylethenyl)benzene **5** (Watanabe *et al.*, 2021). When blue light (447 nm, 30 W) was irradiated on a THF/MeCN solution of **5** in the presence of 5 mol% of pyrene photocatalyst **7** (2.5 mol% per sulfonylethene moiety) and *i*-Pr_2NEt as sacrificial reductant at 323 K for 9 h, the stereoselective reductive desulfonylation proceeded smoothly to produce (*E*,*E*)-**6** in 78% yield. In contrast, during green-light irradiation (514 nm, 30 W), this desulfonylation proceeded only sluggishly. When an ether/pyridine solution of **6** was treated with a THF solution of TBAF (tetrabutylammonium fluoride), desilylation occurred rapidly to give terminal ethyne **8**. After the completion of the desilylation was confirmed by thin-layer chromatography (TLC) analysis, the final step, oxidative cyclization of the resulting terminal bisyne **8**, was carried out in the presence of $Cu(OAc)_2$ in air at 323 K for 3 h. The desired dehydrobenzannulene **1** was obtained as yellow powder after column chromatography on silica gel. The spectroscopic data (^{1}H NMR) were identical to that reported by Ojima *et al.* (1985).

1,3-Bis(2-acetoxy-2-(2-bromophenyl)-1-phenylsulfonylethyl)benzene (3): silica gel (hexane/AcOEt, 6:4); a mixture of diastereomers; white powder; m.p 378–379 K; ^{1}H NMR ($CDCl_3$, 400 MHz): δ 1.86–2.33 (*m*, 6H), 4.27–5.10 (*m*, 2H), 6.57–7.22 (*m*, 8H), 7.26–7.87 (*m*, 14H); ^{13}C{^{1}H} NMR ($CDCl_3$, 101 MHz): δ 20.76, 20.80, 20.9, 21.0, 21.1, 21.2, 70.3, 70.4, 71.0, 71.1, 73.2, 120.8, 127.3, 127.4, 127.6, 127.78, 127.81, 127.9, 128.00, 128.04, 128.2, 128.4, 128.5, 128.6, 128.7, 128.82, 128.85, 128.95, 128.98, 129.05, 129.08, 129.1, 129.16, 129.21, 129.7, 129.8, 129.9, 129.95, 130.04, 130.4, 130.6, 132.58, 132.63, 133.2, 133.3, 133.5, 133.6, 133.7, 133.8, 133.9, 134.0, 135.87, 135.94, 136.0, 136.3, 137.9, 138.9, 139.2, 168.9, 168.97, 169.02, 169.1. HRMS (MALDI–TOF): *m*/*z* [*M* + Na]$^+$ calculated for $C_{38}H_{32}NaO_8S_2$ 860.9803; found: 860.9782.

(*E*,*E*)-1,3-Bis(2-(2-bromophenyl)-1-phenylsulfonylethenyl)benzene (4): silica gel (hexane/AcOEt, 6:4); white powder; m.p 434–435 K; ^{1}H NMR ($CDCl_3$, 400 MHz): δ 6.58–6.60 (*m*, 2H), 6.83–6.85 (*m*, 2H), 6.94–7.00 (*m*, 3H), 7.02 (*t*, 1H, *J* = 1.6 Hz), 7.10–7.14 (*m*, 2H), 7.37–7.41 (*m*, 4H), 7.52–7.60 (*m*, 8H), 8.16 (s, 2H); ^{13}C{^{1}H} NMR ($CDCl_3$, 101 MHz): δ 125.4,

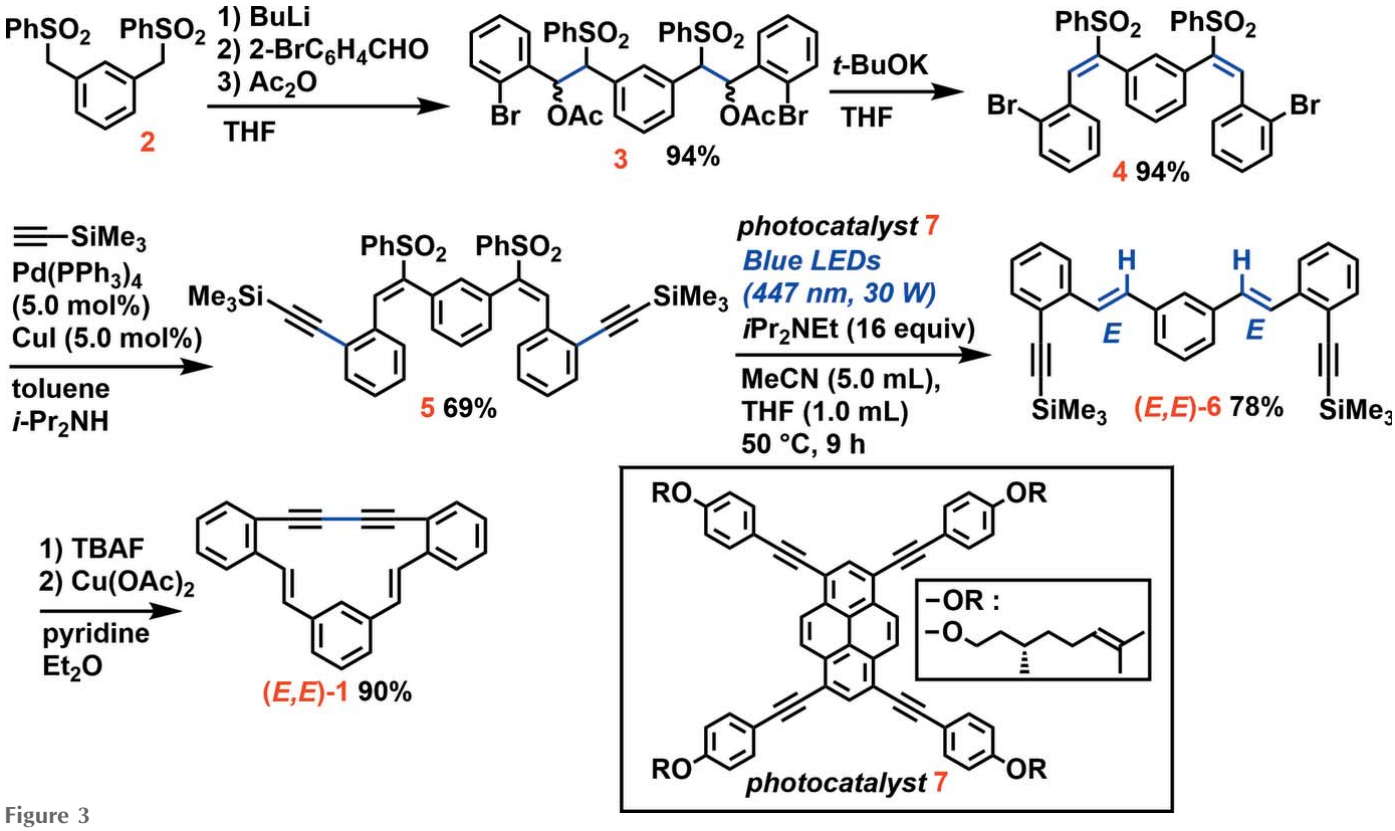

Figure 3
The synthetic route to (*E*,*E*)-**1**.

126.9, 128.4, 128.8, 129.0, 130.5, 130.7, 130.8, 131.6, 133.0, 133.2, 133.4, 133.5, 138.4, 138.5, 142.8. HRMS (MALDI–TOF): *m*/*z* [*M* + Na]$^+$ calculated for $C_{34}H_{24}Br_2NaO_4S_2$ 740.9380; found: 740.9382.

(*E,E*)-1,3-Bis(2-(2-(trimethylsilylethynyl)phenyl)-1-phenylsulfonylethenyl)benzene (5): silica gel (hexane/EtOAc, 8:2); white powder; m.p 444–445 K; ^{1}H NMR ($CDCl_3$, 400 MHz): δ 0.37 (*s*, 18H), 6.64 (*d*, 2H, *J* = 7.6 Hz), 6.92–7.00 (*m*, 5H), 7.06 (*t*, 1H, *J* = 8.0 Hz), 7.19–7.23 (*m*, 2H), 7.35 (*t*, 4H, *J* = 7.8 Hz), 7.48–7.55 (m, 8H), 8.50 (s, 2H); ^{13}C{^{1}H} NMR ($CDCl_3$, 101 MHz): δ 0.09, 102.2, 102.3, 125.5, 127.9, 128.5, 128.8, 128.9, 129.1, 129.5, 131.8, 131.9, 132.8, 133.3, 135.0, 137.6, 139.0, 141.7 (One carbon signal appears to be missing due to overlap). HRMS (MALDI–TOF): *m*/*z* [*M* + Na]$^+$ calculated for $C_{44}H_{42}NaO_4S_2Si_2$ 777.1961; found: 777.1937.

*Synthetic procedure from **5** to (E,E)-**6***

To a round-bottomed flask charged with a magnetic stirrer bar were added ethenyl sulfone **5** (188.5 mg, 0.250 mmol), **7** (15.2 mg, 12.5 µmol), *i*-Pr_2NEt (0.70 mL, 4.0 mmol), MeCN (2.5 mL) and THF (0.5 mL). The flask was placed in a glass water-bath surrounded by blue strip lighting, and blue light was irradiated to the mixture for 9 h. During the photoreaction, the bath temperature was kept at 323–328 K because of heat radiation from the photoreactor. The mixture was evaporated, and the crude product was subjected to flash chromatography (hexane/CH_2Cl_2, 9:1) to afford the desired (*E*,*E*)-**6** (92.6 mg, 0.195 mmol, 78% yield).

(*E,E*)-1,3-Bis{2-[2-(trimethylsilylethynyl)phenyl]ethenyl}benzene [(*E,E*)-6]: yellow powder; m.p 380–381 K; ^{1}H NMR ($CDCl_3$, 400 MHz): δ 0.32 (*s*, 18H), 7.17–7.22 (*m*, 4H), 7.31–7.35 (*m*, 2H), 7.39 (*t*, 1H, *J* = 7.7 Hz), 7.47–7.50 (*m*, 4H), 7.66 (*s*, 1H), 7.68 (*d*, 2H, *J* = 7.7 Hz), 7.73 (*d*, 2H, *J* = 16.4 Hz); ^{13}C{^{1}H} NMR ($CDCl_3$, 101 MHz): δ 0.23, 99.9, 103.7, 124.6, 125.85, 125.91, 127.32, 127.35, 128.9, 129.2, 130.0, 132.9, 138.0, 139.2 (One carbon signal appears to be missing due to overlap). HRMS (MALDI–TOF): *m*/*z* [*M*]$^+$ calculated for $C_{32}H_{34}Si_2$ 474.2199; found: 474.2238.

*Synthetic procedure from (E,E)-**6** to (E,E)-**1***

To an ether (3.3 mL) and pyridine (1.1 mL) solution of **6** (47.5 mg, 0.10 mmol) was added a THF solution of TBAF (1.0 *M*, 0.22 mL, 0.22 mmol) at 273 K, and the mixture was stirred at rt for 3 h. The mixture was added to an ether (3.3 mL) and pyridine (1.1 mL) solution of $Cu(OAc)_2$ (228 mg, 1.3 mmol), and the mixture was stirred at 323 K for 3 h. The mixture was poured into sat. NH_4Cl aqueous solution and AcOEt, and the organic and aqueous layers were separated. The aqueous layer was extracted with AcOEt, and the combined organic layer was washed with water and brine. After drying over $MgSO_4$, the solution was evaporated. The residue was subjected to column chromatography on silica gel (hexane/CH_2Cl_2, 9:1) to provide **1** (29.6 mg, 0.090 mmol, 90% yield).

(*E,E*)-1,3-(3,4:9,10-dibenzododeca-1,11-diene-5,7-diyne-1,12-diyl)benzene ((*E,E*)-1): yellow powder; m.p. 520–521 K; ^{1}H NMR ($CDCl_3$, 400 MHz): δ 7.14 (*d*, 2H, *J* = 16.4 Hz), 7.20–7.24 (*m*, 4H), 7.30 (*dd*, 1H, *J* = 8.2, 6.4 Hz), 7.36–7.40 (*m*, 2H), 7.42–7.44 (*m*, 2H), 7.71 (*d*, 2H, *J* = 8.2 Hz), 8.23 (*d*, 2H, *J* = 16.4 Hz), 8.65 (s, 1H); ^{13}C{^{1}H} NMR ($CDCl_3$, 101 MHz): δ 81.1, 84.9, 121.9, 124.4, 125.0, 127.0, 127.5, 128.87, 128.92, 129.6, 130.7, 130.8, 139.2, 141.7.

The crystal of (*E*,*E*)-**1** used for X-ray diffraction was obtained from slow evaporation of a CH_2Cl_2/hexane solution.

6. Optical properties

To evaluate the electronic effects of the molecular structure of (*E*,*E*)-**1** on its optical properties, UV–Vis absorption and photoluminescence spectra were recorded in $CHCl_3$ (Fig. 4). In the UV–Vis absorption spectrum, (*E*,*E*)-**1** showed the longest and the maximum absorption bands at 377 nm (ε 0.45 $\times$ 10^4 L mol^{-1} cm) and 299 nm (ε 7.4 $\times$ 10^4 L mol^{-1} cm), respectively. The former absorption band was assignable to the HOMO–LUMO transition of (*E*,*E*)-**1** by DFT calculations performed at the B3LYP/6-31G(d) level of theory; 419 nm and *f* = 0.0415 were obtained as the first excitation energy and oscillator strength after calibration by multiplying by 0.96. The DFT calculations also revealed that the HOMO and LUMO of (*E*,*E*)-**1** expanded in the whole molecule (Fig. 5). When UV light was irradiated to the $CHCl_3$ solution of (*E*,*E*)-**1** and in the powdered state, blue and greenish blue-colored emissions were recorded at 468 nm (Φ_F 0.26) and 504 nm (Φ_F 0.24), respectively (Fig. 4).

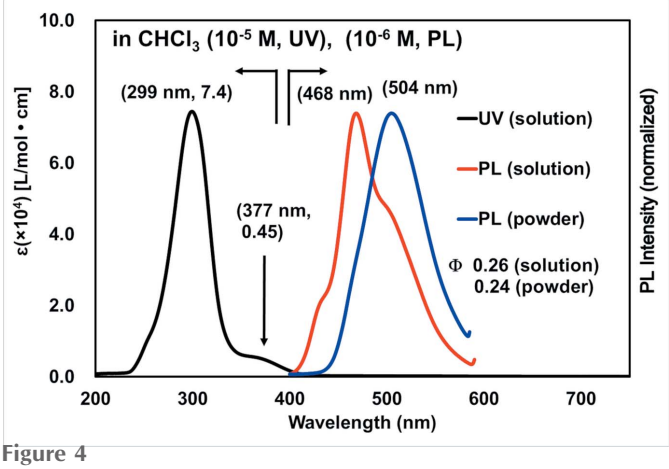

Figure 4
UV–Vis absorption and photoluminescence spectra of (*E*,*E*)-**1**.

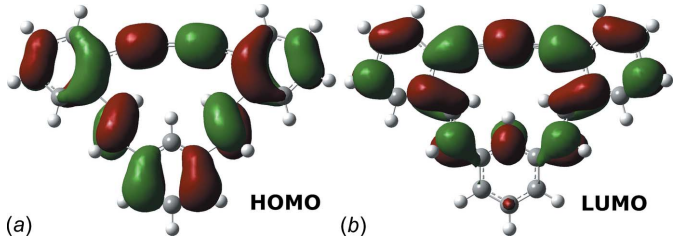

Figure 5
Graphical representation of frontier orbitals (*a*) HOMO and (*b*) LUMO of (*E*,*E*)-**1**.

Table 1
Experimental details.

Crystal data	
Chemical formula	$C_{26}H_{16}$
M_r	328.39
Crystal system, space group	Orthorhombic, $P2_12_12_1$
Temperature (K)	293
a, b, c (Å)	4.6034 (2), 15.1542 (7), 24.1754 (9)
V (Å^3)	1686.50 (12)
Z	4
Radiation type	Mo $K\alpha$
μ (mm^{-1})	0.07
Crystal size (mm)	0.3 × 0.1 × 0.02
Data collection	
Diffractometer	Rigaku VariMax with Saturn
Absorption correction	Multi-scan (*CrysAlis PRO*; Rigaku OD, 2019)
T_{min}, T_{max}	0.739, 1.000
No. of measured, independent and observed [$I > 2\sigma(I)$] reflections	32971, 5357, 4184
R_{int}	0.067
(sin $\theta/\lambda)_{max}$ (Å^{-1})	0.737
Refinement	
$R[F^2 > 2\sigma(F^2)]$, $wR(F^2)$, S	0.058, 0.115, 1.03
No. of reflections	5357
No. of parameters	235
H-atom treatment	H-atom parameters constrained
$\Delta\rho_{max}$, $\Delta\rho_{min}$ (e Å^{-3})	0.25, −0.21
Absolute structure	Undetermined: Flack x obtained using 1343 quotients $[(I^+)-(I^-)]/[(I^+)+(I^-)]$ (Parsons *et al.* (2013)
Absolute structure parameter	−0.4 (10)

Computer programs: *CrysAlis PRO* (Rigaku OD, 2019), *SHELXT* (Sheldrick, 2015*a*), *SHELXL* (Sheldrick, 2015*b*) and *OLEX2* (Dolomanov *et al.*, 2009).

7. Refinement

Crystal data, data collection and structure refinement details are summarized in Table 1. All H atoms were refined using a riding model with d(C—H) = 0.93 Å, U_{iso}(H) = 1.2U_{eq}(C) for aromatic H, 1.00 Å, U_{iso}(H) = 1.2U_{eq}(C) for CH, 0.98 Å.

Acknowledgements

The authors thank Okayama University of Science Research Instruments Center for the X-ray diffraction measurements of the crystal (Rigaku VariMax with Saturn), 400 MHz NMR (Jeol JNM-ECS400 and JNM-ECZ400S), and MALDI–TOF MS (Bruker autoflex speed).

Funding information

Funding for this research was provided by: Grant-in-Aid from Japan Society for the Promotion of Science [JP23K04741 (AO) and JP23K13755 (YO)]; The Okayama Foundation for Science and Technology (AO); Okayama Prefecture Industrial Promotion Foundation (AO); OUS Research Project [OUS-RP-23-2 (AO), OUS-RP-22-4 (YO)]; Wesco Scientific Promotion Foundation (AO); Fukuoka Naohiko Memorial Foundation (YO).

References

Dolomanov, O. V., Bourhis, L. J., Gildea, R. J., Howard, J. A. K. & Puschmann, H. (2009). *J. Appl. Cryst.* **42**, 339–341.
Esser, B., Rominger, F. & Gleiter, R. (2008). *J. Am. Chem. Soc.* **130**, 6716–6717.
Groom, C. R., Bruno, I. J., Lightfoot, M. P. & Ward, S. C. (2016). *Acta Cryst.* B**72**, 171–179.
Karki, S., Karas, L. J., Wang, X., Wu, J. I. & Miljanić, O. Š. (2022). *Cryst. Growth Des.* **22**, 2076–2081.
Ojima, J., Kakumi, H., Kitatani, K., Wada, K., Ejiri, E. & Nakada, T. (1985). *Can. J. Chem.* **63**, 2885–2891.
Orita, A., Taniguchi, H. & Otera, J. (2006). *Chem. Asian J.* **1**, 430–437.
Parsons, S., Flack, H. D. & Wagner, T. (2013). *Acta Cryst.* B**69**, 249–259.
Rigaku OD (2019). *CrysAlis PRO*. Oxford Diffraction Ltd, Yarnton, England.
Sheldrick, G. M. (2015*a*). *Acta Cryst.* A**71**, 3–8.
Sheldrick, G. M. (2015*b*). *Acta Cryst.* C**71**, 3–8.
Shigemitsu, H., Hisaki, I., Kometani, E., Tohnai, N. & Miyata, M. (2012). *Chem. Lett.* **41**, 1535–1537.
Tobe, Y., Kishi, J., Ohki, I. & Sonoda, M. (2003). *J. Org. Chem.* **68**, 3330–3332.
Watanabe, H., Nakajima, K., Ekuni, K., Edagawa, R., Akagi, Y., Okuda, Y., Wakamatsu, K. & Orita, A. (2021). *Synthesis*, **53**, 2984–2994.
Watanabe, H., Takemoto, M., Adachi, K., Okuda, Y., Dakegata, A., Fukuyama, T., Ryu, I., Wakamatsu, K. & Orita, A. (2020). *Chem. Lett.* **49**, 409–412.

supporting information

Acta Cryst. (2023). E**79**, 757-761 [https://doi.org/10.1107/S2056989023006187]

Synthesis, optical properties and crystal structure of (*E*,*E*)-1,3-(3,4:9,10-dibenzododeca-1,11-diene-5,7-diyne-1,12-diyl)benzene

Hikaru Watanabe, Takuma Sato, Michiki Sumita, Mei Shiroyama, Daichi Sugawara, Tomoki Tokuyama, Yasuhiro Okuda, Kan Wakamatsu, Haruo Akashi and Akihiro Orita

Computing details

Data collection: *CrysAlis PRO* (Rigaku OD, 2019); cell refinement: *CrysAlis PRO* (Rigaku OD, 2019); data reduction: *CrysAlis PRO* (Rigaku OD, 2019); program(s) used to solve structure: *SHELXT* (Sheldrick, 2015a); program(s) used to refine structure: *SHELXL* (Sheldrick, 2015b); molecular graphics: Olex2 (Dolomanov *et al.*, 2009); software used to prepare material for publication: Olex2 (Dolomanov *et al.*, 2009).

(*E*,*E*)-1,3-(3,4:9,10-Dibenzododeca-1,11-diene-5,7-diyne-1,12-\ diyl)benzene

Crystal data

$C_{26}H_{16}$
M_r = 328.39
Orthorhombic, $P2_12_12_1$
a = 4.6034 (2) Å
b = 15.1542 (7) Å
c = 24.1754 (9) Å
V = 1686.50 (12) Å^3
Z = 4
$F(000)$ = 688
D_x = 1.293 Mg m^{-3}
Mo $K\alpha$ radiation, λ = 0.71073 Å
Cell parameters from 10472 reflections
θ = 2.1–31.6°
μ = 0.07 mm^{-1}
T = 293 K
Needle, pale yellow
0.3 × 0.1 × 0.02 mm

Data collection

Rigaku VariMax with Saturn diffractometer
Radiation source: fine-focus sealed X-ray tube, Enhance (Mo) X-ray Source
Graphite monochromator
ω scans
Absorption correction: multi-scan (CrysAlisPro; Rigaku OD, 2019)
T_{min} = 0.739, T_{max} = 1.000
32971 measured reflections
5357 independent reflections
4184 reflections with $I > 2\sigma(I)$
R_{int} = 0.067
θ_{max} = 31.6°, θ_{min} = 2.7°
h = −6→6
k = −22→22
l = −35→35

Refinement

Refinement on F^2
Least-squares matrix: full
$R[F^2 > 2\sigma(F^2)]$ = 0.058
$wR(F^2)$ = 0.115
S = 1.03
5357 reflections
235 parameters
0 restraints
Primary atom site location: dual
Hydrogen site location: inferred from neighbouring sites
H-atom parameters constrained
$w = 1/[\sigma^2(F_o^2) + (0.0399P)^2 + 0.5407P]$ where $P = (F_o^2 + 2F_c^2)/3$
$(\Delta/\sigma)_{max} < 0.001$
$\Delta\rho_{max}$ = 0.25 e Å^{-3}

$\Delta\rho_{min}$ = −0.21 e Å^{-3}

Absolute structure: Flack *x* obtained using 1343 quotients [(I^+)-(I^-)]/[(I^+)+(I^-)] (Parsons *et al.* (2013)
Absolute structure parameter: −0.4 (10)

Special details

Geometry. All esds (except the esd in the dihedral angle between two l.s. planes) are estimated using the full covariance matrix. The cell esds are taken into account individually in the estimation of esds in distances, angles and torsion angles; correlations between esds in cell parameters are only used when they are defined by crystal symmetry. An approximate (isotropic) treatment of cell esds is used for estimating esds involving l.s. planes.

Fractional atomic coordinates and isotropic or equivalent isotropic displacement parameters (Å^2)

	x	*y*	*z*	U_{iso}*/U_{eq}
C1	0.2502 (5)	0.45575 (15)	0.56944 (9)	0.0216 (5)
C2	0.4402 (5)	0.47355 (14)	0.61508 (9)	0.0222 (5)
C3	0.5925 (5)	0.49842 (14)	0.65244 (9)	0.0227 (5)
C4	0.7514 (5)	0.53835 (14)	0.69355 (9)	0.0222 (5)
C5	0.8704 (5)	0.58321 (15)	0.72752 (9)	0.0209 (4)
C6	0.9800 (5)	0.64594 (14)	0.76707 (8)	0.0204 (4)
C7	1.1873 (5)	0.62079 (15)	0.80626 (9)	0.0245 (5)
H7	1.262529	0.563841	0.805862	0.029*
C8	1.2806 (6)	0.68078 (16)	0.84569 (9)	0.0274 (5)
H8	1.417729	0.664064	0.871925	0.033*
C9	1.1693 (5)	0.76560 (16)	0.84596 (9)	0.0259 (5)
H9	1.230444	0.805469	0.872792	0.031*
C10	0.9683 (5)	0.79169 (15)	0.80678 (9)	0.0234 (5)
H10	0.898169	0.849244	0.807273	0.028*
C11	0.8687 (5)	0.73307 (14)	0.76650 (8)	0.0202 (4)
C12	0.6595 (5)	0.75690 (15)	0.72402 (9)	0.0242 (5)
H12	0.618597	0.711742	0.699159	0.029*
C13	0.5176 (5)	0.83044 (15)	0.71427 (9)	0.0248 (5)
H13	0.550528	0.878785	0.737125	0.030*
C14	0.3080 (5)	0.83928 (15)	0.66845 (9)	0.0219 (5)
C15	0.1742 (5)	0.91902 (15)	0.65530 (9)	0.0217 (5)
H15	0.218318	0.969579	0.675416	0.026*
C16	−0.0247 (6)	0.92324 (15)	0.61229 (9)	0.0262 (5)
H16	−0.114100	0.976703	0.604104	0.031*
C17	−0.0926 (5)	0.84895 (15)	0.58126 (9)	0.0235 (5)
H17	−0.226582	0.852844	0.552574	0.028*
C18	0.0403 (5)	0.76861 (15)	0.59313 (8)	0.0215 (5)
C19	0.2331 (6)	0.76584 (16)	0.63734 (10)	0.0306 (6)
H19	0.316351	0.711884	0.646541	0.037*
C20	−0.0222 (5)	0.68716 (16)	0.56204 (9)	0.0254 (5)
H20	−0.174216	0.687321	0.536702	0.030*
C21	0.1283 (6)	0.61437 (16)	0.56873 (9)	0.0290 (5)
H21	0.285437	0.620009	0.592654	0.035*
C22	0.0935 (5)	0.52624 (15)	0.54539 (9)	0.0228 (5)
C23	−0.0897 (6)	0.50780 (16)	0.50078 (9)	0.0261 (5)

H23	−0.194796	0.553344	0.484524	0.031*
C24	−0.1173 (6)	0.42325 (17)	0.48049 (10)	0.0291 (5)
H24	−0.238731	0.412385	0.450511	0.035*
C25	0.0346 (6)	0.35453 (16)	0.50444 (10)	0.0311 (6)
H25	0.013435	0.297496	0.490833	0.037*
C26	0.2182 (6)	0.37044 (16)	0.54866 (10)	0.0270 (5)
H26	0.320639	0.324050	0.564593	0.032*

Atomic displacement parameters (Å²)

	U^{11}	U^{22}	U^{33}	U^{12}	U^{13}	U^{23}
C1	0.0218 (11)	0.0244 (11)	0.0187 (10)	−0.0033 (9)	0.0055 (9)	−0.0038 (8)
C2	0.0271 (12)	0.0193 (10)	0.0203 (10)	0.0011 (9)	0.0039 (9)	−0.0021 (8)
C3	0.0274 (12)	0.0174 (10)	0.0232 (10)	0.0019 (9)	0.0039 (9)	−0.0002 (8)
C4	0.0247 (12)	0.0199 (10)	0.0220 (10)	0.0030 (9)	−0.0004 (9)	0.0031 (8)
C5	0.0226 (11)	0.0209 (10)	0.0192 (10)	0.0018 (9)	0.0004 (9)	0.0036 (8)
C6	0.0206 (11)	0.0241 (11)	0.0165 (9)	−0.0035 (9)	0.0015 (9)	0.0015 (8)
C7	0.0251 (12)	0.0250 (11)	0.0233 (11)	−0.0017 (10)	−0.0007 (9)	0.0060 (9)
C8	0.0257 (12)	0.0350 (13)	0.0213 (11)	−0.0047 (11)	−0.0069 (10)	0.0051 (10)
C9	0.0262 (12)	0.0318 (12)	0.0197 (10)	−0.0081 (10)	−0.0022 (9)	−0.0020 (9)
C10	0.0238 (12)	0.0234 (11)	0.0230 (10)	−0.0031 (9)	0.0012 (10)	−0.0005 (8)
C11	0.0205 (11)	0.0234 (11)	0.0167 (9)	−0.0018 (9)	0.0022 (9)	0.0018 (8)
C12	0.0294 (13)	0.0223 (11)	0.0209 (10)	−0.0027 (10)	−0.0046 (10)	−0.0024 (8)
C13	0.0249 (12)	0.0248 (11)	0.0246 (11)	0.0006 (10)	−0.0054 (9)	−0.0055 (9)
C14	0.0206 (11)	0.0246 (11)	0.0204 (10)	0.0011 (9)	0.0010 (9)	−0.0013 (8)
C15	0.0240 (12)	0.0199 (10)	0.0212 (11)	−0.0018 (9)	0.0024 (9)	−0.0004 (8)
C16	0.0337 (14)	0.0212 (11)	0.0237 (11)	0.0051 (11)	0.0000 (11)	0.0048 (9)
C17	0.0259 (12)	0.0269 (12)	0.0177 (10)	0.0017 (10)	−0.0009 (9)	0.0035 (8)
C18	0.0209 (11)	0.0248 (11)	0.0189 (10)	0.0013 (9)	0.0014 (9)	−0.0008 (8)
C19	0.0342 (14)	0.0233 (12)	0.0343 (13)	0.0107 (11)	−0.0111 (11)	−0.0060 (10)
C20	0.0241 (12)	0.0309 (12)	0.0211 (10)	0.0012 (10)	−0.0054 (9)	−0.0037 (9)
C21	0.0379 (15)	0.0264 (12)	0.0225 (11)	−0.0033 (11)	−0.0116 (11)	0.0004 (9)
C22	0.0258 (12)	0.0256 (11)	0.0170 (9)	−0.0047 (10)	0.0033 (9)	−0.0005 (8)
C23	0.0275 (12)	0.0319 (12)	0.0190 (10)	−0.0035 (10)	−0.0010 (9)	−0.0007 (9)
C24	0.0257 (13)	0.0398 (14)	0.0217 (11)	−0.0064 (11)	−0.0001 (10)	−0.0098 (10)
C25	0.0332 (14)	0.0285 (12)	0.0315 (12)	−0.0047 (11)	0.0021 (11)	−0.0139 (10)
C26	0.0274 (13)	0.0269 (12)	0.0267 (11)	0.0008 (10)	0.0021 (10)	−0.0064 (9)

Geometric parameters (Å, º)

C1—C2	1.434 (3)	C14—C19	1.387 (3)
C1—C22	1.414 (3)	C15—H15	0.9300
C1—C26	1.395 (3)	C15—C16	1.387 (3)
C2—C3	1.204 (3)	C16—H16	0.9300
C3—C4	1.374 (3)	C16—C17	1.389 (3)
C4—C5	1.199 (3)	C17—H17	0.9300
C5—C6	1.439 (3)	C17—C18	1.392 (3)
C6—C7	1.398 (3)	C18—C19	1.390 (3)

C6—C11	1.416 (3)	C18—C20	1.474 (3)
C7—H7	0.9300	C19—H19	0.9300
C7—C8	1.386 (3)	C20—H20	0.9300
C8—H8	0.9300	C20—C21	1.313 (3)
C8—C9	1.384 (3)	C21—H21	0.9300
C9—H9	0.9300	C21—C22	1.459 (3)
C9—C10	1.382 (3)	C22—C23	1.397 (3)
C10—H10	0.9300	C23—H23	0.9300
C10—C11	1.396 (3)	C23—C24	1.378 (3)
C11—C12	1.454 (3)	C24—H24	0.9300
C12—H12	0.9300	C24—C25	1.382 (4)
C12—C13	1.313 (3)	C25—H25	0.9300
C13—H13	0.9300	C25—C26	1.384 (3)
C13—C14	1.475 (3)	C26—H26	0.9300
C14—C15	1.393 (3)		

C22—C1—C2	119.0 (2)	C16—C15—C14	120.2 (2)
C26—C1—C2	121.1 (2)	C16—C15—H15	119.9
C26—C1—C22	119.9 (2)	C15—C16—H16	119.5
C3—C2—C1	172.6 (2)	C15—C16—C17	121.1 (2)
C2—C3—C4	172.0 (2)	C17—C16—H16	119.5
C5—C4—C3	171.3 (2)	C16—C17—H17	120.0
C4—C5—C6	171.8 (2)	C16—C17—C18	119.9 (2)
C7—C6—C5	120.6 (2)	C18—C17—H17	120.0
C7—C6—C11	120.5 (2)	C17—C18—C20	122.8 (2)
C11—C6—C5	118.9 (2)	C19—C18—C17	117.7 (2)
C6—C7—H7	120.0	C19—C18—C20	119.5 (2)
C8—C7—C6	119.9 (2)	C14—C19—C18	123.5 (2)
C8—C7—H7	120.0	C14—C19—H19	118.3
C7—C8—H8	120.1	C18—C19—H19	118.3
C9—C8—C7	119.9 (2)	C18—C20—H20	118.7
C9—C8—H8	120.1	C21—C20—C18	122.5 (2)
C8—C9—H9	119.7	C21—C20—H20	118.7
C10—C9—C8	120.7 (2)	C20—C21—H21	114.2
C10—C9—H9	119.7	C20—C21—C22	131.6 (2)
C9—C10—H10	119.5	C22—C21—H21	114.2
C9—C10—C11	121.1 (2)	C1—C22—C21	118.5 (2)
C11—C10—H10	119.5	C23—C22—C1	118.3 (2)
C6—C11—C12	118.6 (2)	C23—C22—C21	123.2 (2)
C10—C11—C6	117.9 (2)	C22—C23—H23	119.5
C10—C11—C12	123.5 (2)	C24—C23—C22	121.1 (2)
C11—C12—H12	114.1	C24—C23—H23	119.5
C13—C12—C11	131.9 (2)	C23—C24—H24	119.8
C13—C12—H12	114.1	C23—C24—C25	120.3 (2)
C12—C13—H13	118.8	C25—C24—H24	119.8
C12—C13—C14	122.5 (2)	C24—C25—H25	119.9
C14—C13—H13	118.8	C24—C25—C26	120.1 (2)
C15—C14—C13	122.6 (2)	C26—C25—H25	119.9

C19—C14—C13	119.8 (2)	C1—C26—H26	119.9
C19—C14—C15	117.5 (2)	C25—C26—C1	120.3 (2)
C14—C15—H15	119.9	C25—C26—H26	119.9